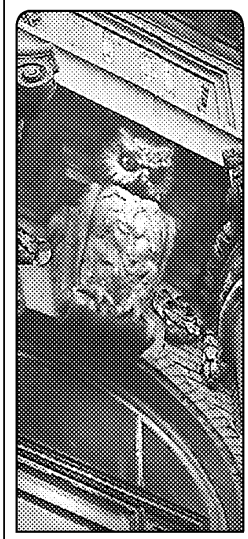

НАУЧНЫЙ ОТДЕЛ

НАНОТЕХНОЛОГИИ, НАНОМАТЕРИАЛЫ И МЕТАМАТЕРИАЛЫ

Известия Саратовского университета. Новая серия. Серия: Физика. 2025. Т. 25, вып. 2. С. 222–229
Izvestiya of Saratov University. Physics, 2025, vol. 25, iss. 2, pp. 222–229
https://fizika.sgu.ru https://doi.org/10.18500/1817-3020-2025-25-2-222-229, EDN: KLFIBO

Article

Characterization of imprinted albumin by molecular modelling and spectroscopy

P. M. Ilicheva✉, I. A. Reshetnik, D. D. Drozd, P. S. Pidenko, N. A. Burmistrova

Saratov State University, 83 Astrakhanskaya St., Saratov 410012, Russia

Polina M. Ilicheva, ilichevapm@gmail.com, https://orcid.org/0000-0002-5825-0032, AuthorID: 1078635
Ivan A. Reshetnik, 0105frenklin@gmail.com, https://orcid.org/0009-0002-0617-2615
Daniil D. Drozd, drozddd@sgu.ru, https://orcid.org/0000-0001-5379-8026, AuthorID: 1037396
Pavel S. Pidenko, pidenkops@gmail.com, https://orcid.org/0000-0001-7771-0957, AuthorID: 879254
Natalia A. Burmistrova, naburmistrova@mail.ru, https://orcid.org/0000-0001-8137-1599, AuthorID: 52279

Abstract. ***Background and Objectives***: Imprinted proteins are promising alternatives to natural recognition systems, such as biological receptors or antibodies. However, the knowledge available on the theoretical study of imprinted proteins as recognition systems is limited. In this study, bovine serum albumin (BSA) is imprinted in the presence of 4-hydroxycoumarin. Change in protein structure is studied by molecular modelling and spectroscopy. ***Materials and Methods*****:** To evaluate the effect of pH on the structural properties of BSA during imprinting, fluorescence 2D and 3D spectroscopy and dynamic light scattering (DLS) combined with molecular dynamics and metadynamics simulations were carried out to monitor the conformational change of the protein matrix. ***Results*****:** Analysis of molecular dynamics simulation has shown that the mechanism of BSA conformational state changes is associated with displacements of molecular domains relative to each other. Based on molecular dynamics data, the values of collective variables have been selected for mapping the free energy of the system. The distance and angle between the centers of mass of domains D1 and D3 have been specified as collective variables. Simulations using the metadynamics method have been performed for 100 ns. As a result, slices of the potential energy surface have been obtained. Analysis of the free energy surface shows that 3.05 nm and 1.53 radian correspond to the minimum energy ($\Delta G = -6.14$ kJ·mol^{-1}). BSA have been studied by fluorescence and DLS. DLS analysis has shown that BSA exists predominantly in monomeric form in solution. In acidic media (pH 3.0) the significant changes of fluorescence properties of BSA have been observed. The results of molecular modelling are consistent with the experimental results. ***Conclusion*****:** An important practical result of this study is that the theoretical study of such molecular systems combined with fluorescence characterization during synthesis can be applied to control imprinting process and to create new imprinted proteins with a wide range of applications.

Keywords: imprinted proteins, molecular dynamics, metadynamics, bovine serum albumin, fluorescence, dynamic light scattering

Acknowledgements: This work was supported by the Russian Science Foundation (project No. 22-16-00102). MD simulation was performed on Saratov State University HPC system.

For citation: Ilicheva P. M., Reshetnik I. A., Drozd D. D., Pidenko P. S., Burmistrova N. A. Characterization of imprinted albumin by molecular modelling and spectroscopy. *Izvestiya of Saratov University. Physics*, 2025, vol. 25, iss. 2, pp. 222–229. https://doi.org/10.18500/1817-3020-2025-25-2-222-229, EDN: KLFIBO

Научная статья
УДК 535.372:535.36

Характеризация импринтированного альбумина методами молекулярного моделирования и спектроскопии

П. М. Ильичева✉, И. А. Решетник, Д. Д. Дрозд, П. С. Пиденко, Н. А. Бурмистрова

Саратовский национальный исследовательский государственный университет имени Н. Г. Чернышевского, Россия, 410012, г. Саратов, ул. Астраханская, д. 83

Ильичева Полина Михайловна, аспирант кафедры общей и неорганической химии Института химии, ilichevapm@gmail.com, https://orcid.org/0000-0002-5825-0032, AuthorID: 1078635
Решетник Иван Александрович, студент-бакалавр кафедры общей и неорганической химии Института химии, 0105frenklin@gmail.com, https://orcid.org/0009-0002-0617-2615
Дрозд Даниил Дмитриевич, кандидат химических наук, доцент кафедры общей и неорганической химии Института химии, drozddd@sgu.ru, https://orcid.org/0000-0001-5379-8026, AuthorID: 1037396
Пиденко Павел Сергеевич, кандидат химических наук, старший научный сотрудник лаборатории неорганической химии Института химии, pidenkops@gmail.com, https://orcid.org/0000-0001-7771-0957, AuthorID: 879254
Бурмистрова Наталия Анатольевна, доктор химических наук, профессор кафедры общей и неорганической химии Института химии, naburmistrova@mail.ru, https://orcid.org/0000-0001-8137-1599, AuthorID: 52279

Аннотация. Импринтированные белки являются многообещающими альтернативами естественным системам распознавания, таким как биологические рецепторы или антитела. Однако имеющиеся знания по теоретическому изучению импринтированных белков как систем распознавания ограничены. В этом исследовании бычий сывороточный альбумин (БСА) был импринтирован в присутствии 4-гидроксикумарина. Для оценки влияния pH на структурные свойства БСА во время импринтинга были проведены флуоресцентная 2D и 3D спектроскопия и динамическое рассеяние света (DLS) в сочетании с моделированием молекулярной динамики и метадинамики для мониторинга конформационного изменения белковой матрицы. В сильнокислых средах наблюдались значительные изменения флуоресцентных свойств BSA. Анализ результатов моделирования показал, что механизм изменения конформационного состояния БСА связан со смещениями молекулярных доменов относительно друг друга. Результаты молекулярного моделирования согласуются с экспериментальными результатами.

Важным практическим результатом данного исследования является то, что теоретическое изучение таких молекулярных систем в сочетании с флуоресцентной характеристикой во время синтеза может быть применено для контроля импринтинга и создания новых импринтированных белков с широким спектром применения.

Ключевые слова: импринтированные белки, молекулярная динамика, метадинамика, бычий сывороточный альбумин, флуоресценция, динамическое рассеяние света

Благодарности: Работа выполнена при финансовой поддержке Российского научного фонда (проект № 22-16-00102). Моделирование МД проводилось на высокопроизводительной вычислительной системе Саратовского национального исследовательского государственного университета имени Н. Г. Чернышевского.

Для цитирования: Ilicheva P. M., Reshetnik I. A., Drozd D. D., Pidenko P. S., Burmistrova N. A. Characterization of imprinted albumin by molecular modelling and spectroscopy [*Ильичева П. М., Решетник И. А., Дрозд Д. Д., Пиденко П. С., Бурмистрова Н. А.* Характеризация импринтированного альбумина методами молекулярного моделирования и спектроскопии] // Известия Саратовского университета. Новая серия. Серия: Физика. 2025. Т. 25, вып. 2. С. 222–229. https://doi.org/10.18500/1817-3020-2025-25-2-222-229, EDN: KLFIBO

Introduction

Developing synthetic recognition systems is a widespread direction of analytical chemistry. The most attractive way to replace natural biological recognition systems is based on applying molecularly imprinted polymers (MIPs) due to their relative stability and low cost [1, 2]. It is well-known that there are problems related to the polymer matrix homogeneity, such as the deep location and inaccessibility of binding sites during polymerization in bulk that may arise when developing MIPs [3]. To overcome this problem, surface imprinting methods, such as obtaining molecular imprints on the surface of inorganic sorbents or in a layer of polyelectrolytes applied to a substrate, are widely used [2, 3]. Such imprinted films are widely used in biosensors [4–7], and the materials based on molecularly imprinted inorganic carriers are mainly used in solid-phase extraction [8–10]. Nevertheless, these methods have limitations of applicability in aqueous solutions, which is a key disadvantage of their applicability in biological systems.

The development of protein imprinting technology that combines the properties of natural protein matrix and the unique characteristics of imprinted materials opens new horizons for biomedical applications, including design of artificial enzymes and biocatalysis [4, 11, 12]. Formation of molecular imprints on the protein surface (also known as conformational modification, imprinted proteins (IPs), bioimprinting, enzymatic memory, etc.) allows to control various functions of native proteins. The

relevance of developing IPs is that they can bind with various medicinal and bioactive substances, becoming drug carriers. Imprinting of bovine serum albumin (BSA) in the presence of 4-hydroxycoumarin (4-HC) have been described recently [13]. Despite the obvious promise of their application, there is no comprehensive experimental characterization of IPs during synthesis as well as structural information about IPs formation that could help to precisely control their properties.

In this work, we describe the structural and spectral characteristics of BSA imprinted in the presence of 4-HC to study how pH during synthesis effects the resulting IPs structure. We evaluate structural changes in BSA induced by pH changes via steady-state and time-resolved fluorescence combined with molecular dynamics (MD) and metadynamics techniques. The variability of the protein matrix and template molecules can allow to create new IPs with a wide range of applications.

Experimental Section

1.1. Materials

BSA, 4–HC (98%) and glutaraldehyde (GA) (50 wt% aqueous solution) were purchased from Merck (Merck KGaA, Germany), phosphate-buffered saline (PBS) was prepared from tablets (Rosmedbio LLC, Russia). All solutions were made using deionized water with specific resistivity higher than 18.2 MΩ cm^{-1} from the Milli-Q (Millipore, USA). The purity of all other chemicals was analytical grade. Disposable PD–10 gel filtration desalting columns (GE Healthcare UK Ltd., UK), 30 000 MWCO Dispo-Biodialyzer (Biodialyzer, JET Bio-Filtration Co. Ltd., China) for centrifuge concentration and 10 000 MWCO dialysis bags (Thermo Scientific Inc., USA) were used to carry out the purification.

1.2. Imprinting procedure

The imprinting of BSA was carried out according to the standard technique of imprinting described by Liu et al. [14] with some modifications. To summarize, 1 mg of BSA was dissolved in 1 mL of water and incubated at room-temperature (RT); the mixture stirred for 10 min. Subsequently, the pH of protein solution was adjusted to pH 3.0 by adding the required quantity of hydrochloric acid and stirred for 10 min. 100 μL of 200 μg·mL^{-1} ethanol solution of 4–HC (template molecule – the molecule that will be imprinted) was added to protein solution and incubate (RT) with the mixture stirred for 20 min. Then mixture pH was adjusted to 9 with 0.1 M solution of NaOH to cross-link the protein:template complex with 100 μL of glutaraldehyde solution (1% v/v in H_2O, (GA)). The final mixture consisting of IPs and unreacted components (pH 8) was placed into fridge (4°C), stirred for 30 min and left for 18 h without stirring. None imprinted protein (nIP) was obtained using a similar procedure without the template addition step.

1.3. Spectroscopic measurements

Fluorescence spectra were recorded using Cary Eclipse Fluorescence Spectrophotometer (Agilent Technologies, USA) in the spectral range of 250–550 nm with the resolution of 1 nm and optical path length of 1 cm. The intrinsic protein fluorescence of BSA was recorded using excitation at 290 nm. Fluorescence lifetime measurements were performed using DeltaPro TCSPC Lifetime Fluorometer (Horiba Scientific, UK). Decay curves were approximated by the 3-exponent subject to IRF via Horiba EzTime software. Dynamic light scattering (DLS) measurements were carried out using a Zetasizer Advance Ultra (Malvern Panalytical, UK) equipment complex for studying the characteristics of dispersed systems.

1.4. Computational details

The crystallographic structure of BSA (PDB ID: 4F5S) at the resolution of 2.47 Å was downloaded from the Protein Data Bank database [15]. For calculations, we considered the monomeric form of BSA. Protein structure preparation included addition of hydrogen atoms and missing amino acid side chains, removal of solvent molecules, and adjustment of the protonation state. The protonation state was adjusted to simulate a lower pH value (3.0). All lysine (Lys), arginine (Arg), and histidine (His) residues were positively charged. All-atom MD simulation was performed using the GROMACS package v.4.5.410 [16]. Protein parameters were generated using OPLS-AA force field [17]. Protein was immersed in a cubic box (19×19×19 nm^3) containing 235580 water molecules with a 4.5 nm buffer zone from the surface of the protein. System was solvated with TIP3P water model. The Total number of atoms was 716075. Charge neutralization was carried out by adding 99 chloride ions. System preparation included minimization and equilibration stages. We ran three replicate equilibrations, with randomized initial velocities. Finally, 40 ns of production MD runs were performed allowing all molecules to move in all directions.

Well-tempered metadynamics simulations were performed to reconstruct the free energy surface

(FES) of the system. The metadynamics simulations were performed with two collective variables. A metadynamic potential of 1 kJ/mol was applied every 500 steps. The potential width was chosen based on an unbiased run and was 0.04 radians for the collective variable (CV), corresponding to angle, and 0.08 nm for the CV, corresponding to distance. The bias factor was set to 20. FES was built based on the reweighted data. The simulation time was 100 ns.

2. Results and Discussion

2.1. Conformational changes of BSA under acidic conditions

The initial stage of imprinting process is the protonation of amino acid residues of a protein under acidic conditions (pH 3.0). pH-dependent changes in the protonation state of protein can affect almost all molecular mechanisms related to protein functions and stability. Ignoring protonation changes can be misleading in predicting the binding sites of molecules due to the large effect of desolvation of buried charged groups and stronger interactions inside the protein interior. In this regard, we set the required protonated states of titratable amino acid residues (Asp, Glu, His, Lys, Arg) of BSA at pH 3.0 according to their acidity constants before simulation. The total charge of BSA molecule at pH 7.4 and at pH 3.0 was −17 and +99, respectively. It should be noted that the calculated positive charge is in good agreement with the previously reported charge value of BSA at low pH [18–21].

Molecular modelling has shown that the mechanism of BSA conformational state changes is associated with displacements of molecular domains relative to each other (Fig. 1). When an individual protein is highly charged, strong intramolecular electrostatic repulsions cause partial unfolding of the protein. This is due to significant displacement of D3 domain in relation to the original position. According to some studies, partial unfolding of BSA is associated precisely with an increase of the average distance between D1 and D3 domains [19, 20]. Large changes of root mean square deviation (RMSD) indicate that BSA is undergoing a large conformational change during the simulation (Fig. 1).

MD simulations were performed for several tens of nanoseconds. Although extensive by current standards, these computational times were not sufficient to sample the large-scale conformational changes which typically occur in hundreds of microseconds and were only suggestive of a possible pH destabilization [22]. Therefore, we used metadynamics which successfully applied for mapping the FES of biomolecular processes [23]. Metadynamics is an atomistic simulation technique that allows, within the same framework, acceleration of rare events and estimation of the free energy of complex molecular systems. Metadynamics makes it possible to accelerate conformational transitions between metastable states, broadening the scope of molecular dynamics simulations. It is based on iteratively 'filling' the potential energy of the system by a sum of Gaussians centered along the trajectory followed by a suitably chosen set of collective variables (CVs), thereby forcing the system to migrate from one minimum to the next.

In Fig. 2, the free-energy landscape is represented as a function of two CVs: the average distance and the angle between D1 and D3 domains. The free-energy landscape that we calculated illustrates explicitly the presence of one distinct state of BSA: 3.05 nm and 1.53 radian correspond to the minimum energy (ΔG = –6.14 kJ·mol^{-1}). This representation reveals the organization of the free-energy landscape, with a deep minimum corresponding to F-isoform of BSA.

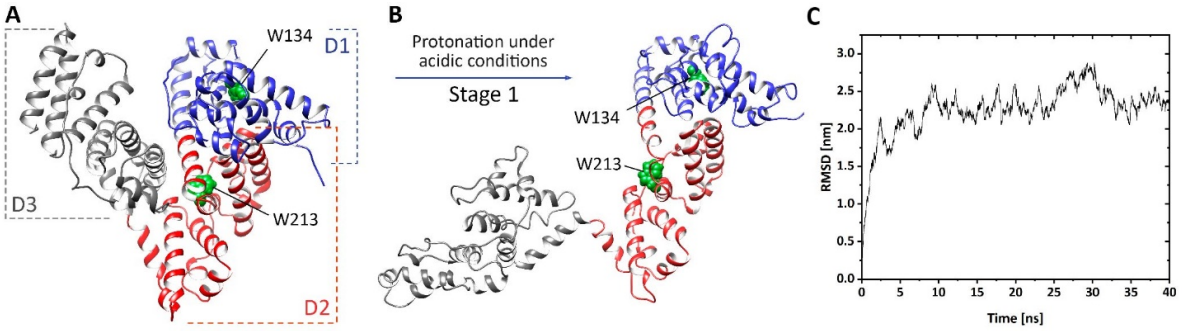

Fig. 1. Molecular structure of BSA at different IPs synthesis stages: A – Native structure corresponds to PDB ID 4F5S; three main domains are shown in blue, red, and grey, respectively; tryptophan residues are shown in green; B – Protein protonation (pH 3.0) is associated with the event of new conformation formation; C – Average RMSD of C-alphas of BSA during molecular dynamics simulation

This result is confirmed by the analysis of the spectral parameters of BSA.

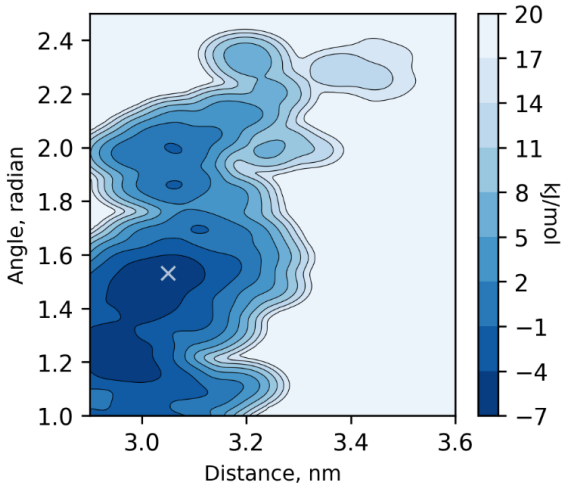

Fig. 2. FES of free BSA during metadynamics simulation (color online)

2.2. Spectral characterization of free BSA at various pH

A feature of intrinsic protein fluorescence is the high sensitivity of tryptophan (Trp) to its local environment that can change in response to conformational changes, subunit association, or denaturation. The emission of indole group of Trp may be blue shifted if the group is buried within a native protein, and its emission may shift to longer wavelengths (red shift) when the protein is unfolded [24]. The fluorescent properties of BSA are due to the existence of two Trp residues in different positions, one located on the protein surface in domain I (Trp-134), more exposed to the hydrophilic environment, and the other one in the hydrophobic pocket in domain II (Trp-213). Fluorescence spectroscopy was carried out to investigate the conformational changes of BSA molecules as a function of pH (Fig. 3A). At pH 5 – near the isoelectric point (∼4.8) of BSA – fluorescence has maximal intensity. When the pH shifted (to more acidic or alkaline range), a decrease in the intensity and blue shift of fluorescence maximum were observed, reflecting the predominantly nonpolar character of the indole environment. The relatively compact molecular structure ensures efficient energy transfer from phenylalanine (Phe) and tyrosine (Tyr) to Trp at pH 5 (near the isoelectric point). Trp electronic distribution in the ground state differs between protonated (low pH) and non-protonated (high pH) states. The presence of hydrogen on the Trp quenches the amino acid fluorescence excitation intensity, which reduces the final protein fluorescence intensity. The interdomain separation caused the exposure of the Trp residues that were buried between domains and resulted in an increase in the solvent accessible surface area (SASA). Trp residue emission can be described with three fluorescence lifetimes, and it is not possible, in BSA, to assign a specific lifetime to a specific Trp residue [25]. Two different lifetimes (∼0.5 and ∼3.1 ns) are due to the emission from two nearly identical electronic absorption transitions $1L_a$ and $1L_b$ of Trp. A third fluorescence lifetime of Trp (ranging from 6 to 9 ns in human and bovine serum albumins) is a result of the interactions of the surrounding with Trp. In all cases, three exponential functions were required to fit the data and the lifetime components (τ_i) were 2.84 ns, 6.31 ns, and 0.16 ns for pH 5.0 (Table). The χ_2 value was close to 1 for

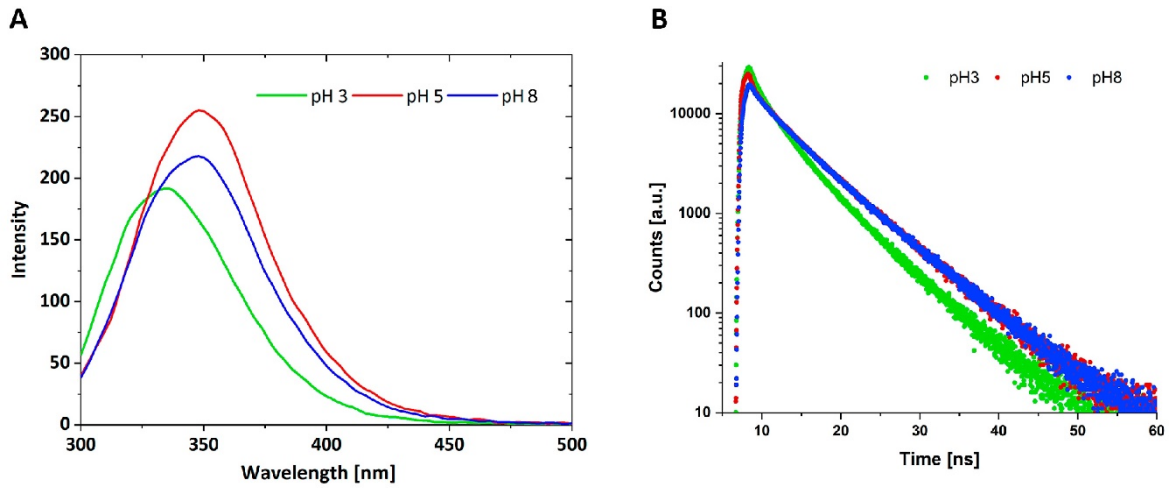

Fig. 3. pH-dependent spectra of the BSA: A – fluorescence spectra, B – fluorescence decay curves (color online)

all cases, which validates our model. pH shifting induces small but significant modifications in lifetime values: 2.31 ns (–19% at pH 3.0) and 2.97 ns (+5% at pH 8.0) for τ_1; 5.51 ns (–13% for pH 3.0) and 6.44 ns (+2% at pH 8.0) for τ_2; 0.29 ns (+81% at pH 3.0) and 0.27 ns (+69% at pH 8.0) for τ_3. When pH shifts from 5.0 to 3.0 the average lifetime drops about 20%. The protonation of Trp decreases fluorescence lifetime values, a phenomenon identical to that observed with fluorescence excitation intensities. Thus, we have a correlation between Trp protonation and fluorescence intensity and lifetime values.

DLS was used to reveal changes in aggregate formation in BSA solutions with different pH. As can be seen from Fig. 4, aggregation did occur for the partially unfolded form of BSA. The authors of Ref.[19] also suggested the coexistence of monomers (~70–80%) and dimers (~15–25%) at a similar pH value measured by high-performance liquid chromatography. The results of MD simulation confirmed DLS results, that shows that the exposure of the hydrophobic surface under acidic conditions can mediate BSA dimerization, since the protein tends to hide exposed amino acids by binding to another monomer.

2.3. Spectral characterization of BSA during IPs synthesis (BSA in the presence of 4-HC)

When BSA makes conformational transition with lowering the solution pH to 3.0, the fluorescence intensity decreases, and the spectrum blue shifts from 350 nm to 338 nm (Fig. 5F). The excitation–emission matrix (EEM) of BSA has one emission spot at pH 3.0 (λex = 260–290 nm) (Fig. 5B). Adding 4-HC leads to decreasing the fluorescence intensity and red shifting from 338 nm to 342 nm. The red shift of the fluorescence maximum indicates the process of association between the protein matrix and template molecules. In the 3-dimensional spectral analysis for BSA in the presence of 4-HC, overlapping of protein and template signals were found (Fig. 5). The fluorescence spectrum of 4-HC with an excitation range of 230–320 nm and local emission maxima at 350–375 nm was observed. When pH increases to 8.0, the red-shift and decrease of the fluorescence intensity were observed; EEMs shows an intensive 4-HC signal, which relates to additional binding sites formation. Cross-linking leads to a significant decrease of the fluorescence intensity due to strong absorbance of GA around 280 nm. The emission maximum of final IPs after removal of templates had one emission spot, which is close to individual BSA at pH 3.0, indicates that the final IPs had the same conformation of BSA.

Thus, the conformational differences between free at pH 3.0 and the final imprinted protein are insignificant. We hypothesizes the stability of protein matrix increases after association under acidic

Table. Fluorescence Decay Fitting Parameters for BSA

pH	τ_1, ns	τ_2, ns	τ_3, ns	$<\tau>$, ns	χ_2
3.0	2.31	5.51	0.29	4.70	1.11
5.0	2.84	6.31	0.16	5.88	1.07
8.0	2.97	6.44	0.27	5.95	0.99

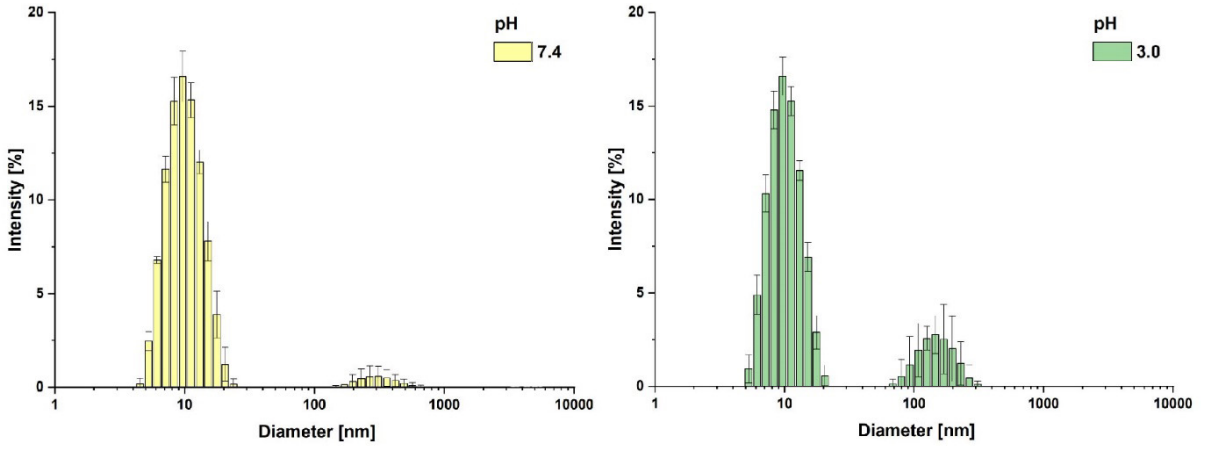

Fig. 4. Particle size distribution of BSA (C = 1 mg/mL) depending on pH (color online)

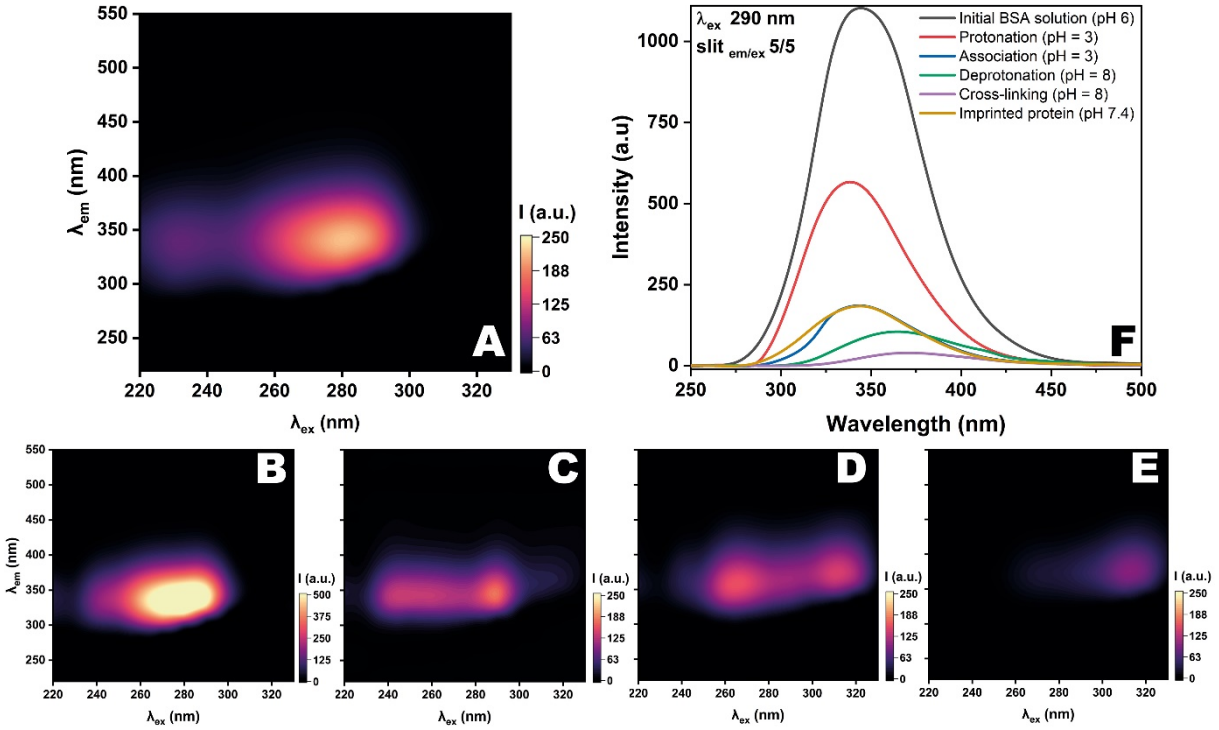

Fig. 5. Fluorescence heatmaps during synthesis: A – purified IPs, B – BSA at pH 3.0, C – BSA-4-HC at pH 3.0, D – BSA-4-HC at pH 8.0, E – BSA-4-HC at pH 8.0 with GA, F – 2D fluorescence spectra during synthesis (color online)

conditions during synthesis. After association the protein with new protonation state at pH 8.0 cannot change conformation due to partial shielding of the functional amino acids. The binding interaction drives the protein towards a new conformation of only local binding regions that become more complementary to template molecules.

Conclusions

In this paper, an approach based on fluorescence spectroscopy combined with molecular modelling has been proposed to characterize the protein matrix during imprinting process. The results of the study of the influence of synthesis conditions on the BSA structure have shown that acidic conditions on the first stage of synthesis can increase the solvent accessible surface area of protein, adjust protonation state and stabilize association with template molecules.

An important practical result of this study is that the theoretical study of such molecular systems combined with fluorescence characterization during synthesis can be applied to control the IPs formation and to create new IPs with a wide range of applications.

References

1. Ramanavicius S., Jagminas A., Ramanavicius A. Advances in Molecularly Imprinted Polymers Based Affinity Sensors (Review). *Polymers*, 2021, vol. 13, iss. 6, art. 974. https://doi.org/10.3390/polym13060974
2. Cormack P., Elorza A. Molecularly imprinted polymers: synthesis and characterisation. *J. Chromatogr. B*, 2004, vol. 804, iss. 1, pp. 173–182. https://doi.org/10.1016/j.jchromb.2004.02.013
3. Piletsky S. *Molecular Imprinting of Polymers*. Boca Raton, CRC Press, 2006. 220 p.
4. Pilvenyte G., Ratautaite V., Boguzaite R., Ramanavicius A., Viter R., Ramanavicius S. Molecularly Imprinted Polymers for the Determination of Cancer Biomarkers. *Int. J. Mol. Sci.*, 2023, vol. 24, iss. 4, art. 4105. https://doi.org/10.3390/ijms24044105
5. Kul A., Budak F., Cetinkaya A., Kaya S., Al S., Sagirli O., Ozkan S. Fabrication of a molecularly imprinted polymer-based electrochemical sensor for the selective assay of antipsychotic drug clozapine and performance comparison with LC–MS/MS. *Talanta*, 2025, vol. 281, art. 126810. https://doi.org/10.1016/j.talanta.2024.126810
6. Barzallo D., Palacio E., Ferrer L., Taboada Sotomayor M. del P. All-in-one spot test method for tetracycline using molecularly imprinted polymer-coated paper integrated into a portable 3D printed platform with smartphone-based fluorescent detection.

Talanta, 2025, vol. 281, art. 126856. https://doi.org/10.1016/j.talanta.2024.126856

7. Liu Y., Meng X., Ma Z., Gu H., Luo X., Yin X., Yi H., Chen Y. Hybrid recognition-enabled ratiometric electrochemical sensing of Staphylococcus aureus via in-situ growth of MOF/Ti3C2Tx-MXene and a self-reporting bacterial imprinted polymer. *Food Chem.*, 2025, vol. 463, pt. 4, art. 141496. https://doi.org/10.1016/j.foodchem.2024.141496
8. Govindarajan V., Karthick T., Muthuraman M. Selective extraction of Quercetin from rose petal extracts using poly (acrylamide-co-ethylene glycol dimethylacrylate) based magnetic molecularly imprinted polymer. *J. Mol. Struct.*, 2025, vol. 1321, art. 140188. https://doi.org/10.1016/j.molstruc.2024.140188
9. Liu M., Xiang B., Li H., He X., Li H., Du K., Li X. A sustainable Poly (deep eutectic solvents) based molecular imprinting strategy with experimental and theoretical elucidation: Application for removal of atrazine in agricultural wastewater. *Sep. Purif. Technol.*, 2025, vol. 353, art. 128637. https://doi.org/10.1016/j.seppur.2024.128637
10. Sun R., Fang Y., Li Y., Wie J., Jiao T., Chen Q., Guo Z., Chen X., Chen X. Molecularly imprinted polymers-coated magnetic covalent organic frameworks for efficient solid-phase extraction of sulfonamides in fish. *Food Chem.*, 2025, vol. 462, no. 3, art. 141007. https://doi.org/10.1016/j.foodchem.2024.141007
11. Zhang Y., Wang Q., Zhao X., Ma Y., Zhang H., Pan G. Molecularly imprinted nanomaterials with stimuli responsiveness for applications in biomedicine. *Molecules*, 2023, vol. 28 no. 3, art. 918. https://doi.org/10.3390/molecules28030918
12. Xu J., Miao H., Wang J., Pan G. Molecularly Imprinted Synthetic Antibodies: From Chemical Design to Biomedical Applications. *Small*, 2020, vol. 16, no. 26, art. e1906644. https://doi.org/10.1002/smll.201906644
13. Presnyakov K. Yu., Ilicheva P. M., Tsyupka D. V., Khudina E., Pozharov M. A., Pidenko P. S., Burmistrova N. A. Dummy-template imprinted bovine serum albumin for extraction of zearalenone. *Micro-Chim Acta*, 2024, vol. 191, art. 767. https://doi.org/10.1007/s00604-024-06790-7
14. Liu J., Zhang K., Ren X., Luo G., Shen J. Bioimprinted protein exhibits glutathione peroxidase activity. *Anal. Chim. Acta*, 2004, vol. 504, iss. 1, art. 185–189. https://doi.org/10.1016/S0003-2670(03)00763-3
15. Berman H., Westbrook J., Feng Z., Gilliland G., Bhat T., Weissig H., Shindyalov I., Bourne P. The Protein Data Bank. *Nucleic Acids Res.*, 2000, vol. 28, iss. 1, pp. 235–242. https://doi.org/10.1093/nar/28.1.235
16. Hess B., Kutzner C., van der Spoel D., Lindahl E. GROMACS 4: Algorithms for Highly Efficient, Load-Balanced, and Scalable Molecular Simulation. *J. Chem. Theory Comput.*, 2008, vol. 4, iss. 3, pp. 435–447. https://doi.org/10.1021/ct700301q
17. Jorgensen W., Maxwell D., Tirado-Rives J. Development and Testing of the OPLS All-Atom Force Field on Conformational Energetics and Properties of Organic Liquids. *J. Am. Chem. Soc.*, 1996, vol. 118, iss. 45, pp. 11225–11236. https://doi.org/10.1021/ja9621760
18. Kumar Srivastav A., Gupta S., Kumar U. A molecular simulation approach towards the development of universal nanocarriers by studying the pH- and electrostatic-driven changes in the dynamic structure of albumin. *RSC Adv.*, 2020, vol. 10, iss. 13, pp. 13451–13459. https://doi.org/10.1039/D0RA00803F
19. Scanavachi G., Espinosa Y., Yoneda J., Rial R., Ruso J., Itri R. Aggregation features of partially unfolded bovine serum albumin modulated by hydrogenated and fluorinated surfactants: Molecular dynamics insights and experimental approaches. *J. Colloid Interface Sci.*, 2020, vol. 572, no. 1, pp. 9–21. https://doi.org/10.1016/j.jcis.2020.03.059
20. Baler K., Martin O., Carignano M., Ameer G., Vila J., Szleifer I. Electrostatic Unfolding and Interactions of Albumin Driven by pH Changes: A Molecular Dynamics Study. *J. Phys. Chem. B*, 2014, vol. 118, iss. 4, pp. 921–930. https://doi.org/10.1021/jp409936v
21. Ilicheva P. M., Fedotova E. S., Presnyakov K. Yu., Grinev V. S., Pidenko P. S., Burmistrova N. A. Theoretical design of imprinted albumin against foodborne toxins. *Mol. Syst. Des. Eng.*, 2024, vol. 9, iss. 5, pp. 456–463. https://doi.org/10.1039/D3ME00179B
22. Prakash M., Barducci A., Parrinello M. Probing the Mechanism of pH-Induced Large-Scale Conformational Changes in Dengue Virus Envelope Protein Using Atomistic Simulations. *Biophys. J.*, 2010, vol. 99, iss. 2, pp. 588–594. https://doi.org/10.1016/j.bpj.2010.04.024
23. Berteotti A., Cavalli A., Branduardi D., Gervasio F., Recanatini M., Parrinello M. Protein Conformational Transitions: The Closure Mechanism of a Kinase Explored by Atomistic Simulations. *J. Am. Chem. Soc.*, 2009, vol. 131, iss. 1, pp. 244–250. https://doi.org/10.1021/ja806846q
24. Lakowicz J. *Principles of Fluorescence Spectroscopy*. New York, Springer, 2006. 954 p.
25. Albani J. Origin of Tryptophan Fluorescence Lifetimes. Part 2: Fluorescence Lifetimes Origin of Tryptophan in Proteins. *J. Fluoresc.*, 2014, vol. 24, pp. 105–117. https://doi.org/10.1007/s10895-013-1274-y

Поступила в редакцию 27.11.2024; одобрена после рецензирования 24.12.2024;
принята к публикации 20.01.2025; опубликована 30.06.2025

The article was submitted 27.11.2024; approved after reviewing 24.12.2024;
accepted for publication 20.01.2025; published 30.06.2025